Universiteit
Leiden
The Netherlands

Ab initio molecular dynamics calculations on reactions of molecules with metal surfaces

Nattino, F.

Citation
Nattino, F. (2015, October 28). *Ab initio molecular dynamics calculations on reactions of molecules with metal surfaces*. Retrieved from https://hdl.handle.net/1887/35980

Version:	Corrected Publisher's Version
License:	Licence agreement concerning inclusion of doctoral thesis in the Institutional Repository of the University of Leiden
Downloaded from:	https://hdl.handle.net/1887/35980

Note: To cite this publication please use the final published version (if applicable).

Cover Page

Universiteit Leiden

The handle http://hdl.handle.net/1887/35980 holds various files of this Leiden University dissertation

Author: Nattino, Francesco
Title: Ab initio molecular dynamics calculations on reactions of molecules with metal surfaces
Issue Date: 2015-10-28

Chapter 5

Ab Initio Molecular Dynamics Calculations versus Quantum-State Resolved Experiments on CHD_3 + Pt(111): New Insights into a Prototypical Gas-Surface Reaction

This chapter is based on:

F. Nattino, H. Ueta, H. Chadwick, M. E. van Reijzen, R. D. Beck, B. Jackson, M. C. van Hemert, and G. J. Kroes, J. Phys. Chem. Lett. **5**, 1294 (2014).

Abstract

The dissociative chemisorption of methane on metal surfaces is of fundamental and practical interest, being a rate-limiting step in the steam reforming process. The reaction is best modeled with quantum dynamics calculations, but these are currently not guaranteed to produce accurate results because they rely on potential energy surfaces based on untested density functionals, and on untested dynamical approximations. To

help overcome these limitations, here we present for the first time statistically accurate reaction probabilities obtained with *ab initio* molecular dynamics (AIMD) for a polyatomic gas phase molecule reacting with a metal surface. Using a general purpose density functional, the AIMD reaction probabilities are in semi-quantitative agreement with new quantum-state resolved experiments on CHD_3 + Pt(111). The comparison suggests the use of the sudden approximation for treating the rotations even though CHD_3 has large rotational constants, and yields an estimated reaction barrier of 0.9 eV for CH_4 + Pt(111).

5.1 Introduction

The steam reforming process, in which methane and water react over a Ni catalyst, is the main commercial source of molecular hydrogen. The dissociation (or dissociative chemisorption) of CH_4 on the catalyst into CH_3(ad) + H(ad) is a rate-determining step of the full process [1]. Moreover, dissociation of methane on metal surfaces is of fundamental interest [2–13]. Already from early molecular beam experiments it is known that vibration is very effective in promoting reactivity [3,4,14]. More recently, it has been shown that the reaction is mode specific, i.e., the degree to which energizing the molecule promotes reaction depends on whether the energy is put in translation or vibration, and even on which vibration it is put in (vibrational mode-specificity) [5–8]. These observations, which have been explained qualitatively on the basis of different models [9, 15], rule out the application of fully statistical models. For some vibrational modes, the vibrational efficacy, which measures how effective putting energy into vibration is at promoting reaction relative to increasing the incidence energy (E_i), is even larger than one [7, 10]. In addition, the dissociation of partially deuterated molecules shows bond-selectivity; for instance, in CHD_3, the CH bond can be selectively broken upon excitation to an appropriate initial vibrational state [11, 12]. Finally, dissociative chemisorption of methane on metal surfaces represents a current frontier in the theoretical description of the dynamics of reactions of gas phase molecules on metal surfaces [15–24], with much current efforts now being aimed at achieving an accurate description of this reaction

through high-dimensional quantum dynamics calculations [16, 23, 24].

A wealth of experiments exist for the methane + Pt(111) system [3, 8, 12, 17, 25–29]. There has been considerable debate [2, 25] concerning the importance of tunneling in this and similar systems. Recent calculations [17, 23, 30] suggest only a minor role for tunneling under the conditions addressed by us. Research on Ni [31] and on Pt [17] surfaces suggests that the dissociation of methane should proceed through a direct mechanism under both thermal and hyperthermal conditions on these surfaces. This suggests the possibility to accurately model experiments relevant to both kinetics and dynamics with a unified approach. Harrison and coworkers have indeed shown [17] that a dynamically biased semi-empirical statistical model yields an accurate description of a large range of experiments. However, this model cannot describe that, as also observed for CH_4 + Pt(111) [8,26,27], the extent to which putting energy into vibration promotes reaction depends on which vibrational state is excited. The model also does not yield the minimum reaction barrier height (E_b), which would be useful for testing new electronic structure methods that are potentially more accurate than the present state-of-the-art method for computing potential energy surfaces (PESs) for molecule-metal surface reactions (density functional theory (DFT) at the generalized gradient approximation (GGA) level) [32]. The DFT-GGA method is known to yield E_b with an accuracy no better than 3.8 kcal/mol for gas phase reactions [33, 34], with GGA functionals both underestimating and overestimating E_b for gas-metal surface reactions [35], while adsorption energies on metal surfaces exhibit similar lack of accuracy [36]. An accurate value of E_b is also relevant to accurately modeling the steam reforming reaction over a Pt(111) surface, as kinetics calculations of rates of heterogeneously catalyzed processes require reaction barrier heights as input parameters [1].

Within the appropriate level of dynamical theory and if an accurate PES is available, dynamics calculations can in principle solve all of the above problems and yield a consistently accurate description of all experiments described above. Dynamics calculations and their comparison to supersonic molecular beam experiments directly test whether the PES contains an accurate description of E_b and of the couplings of the molecule's

and surface atoms' vibrations to the reaction coordinate. The quasi-classical trajectory (QCT) method (trajectory method with zero-point energy (ZPE) imparted to all molecular vibrational modes) is cheap to use, but with this method artificial energy flow between vibrations of similar frequency can occur even in the isolated molecule [22]. This could hamper the accurate calculation of vibrational efficacies, and explains that vibrational efficacies computed with the QCT method for CH_4 + Ni(111) are too low when compared with experiments and results of quantum dynamics (QD) calculations [15,22]. It would therefore be best to use QD to describe methane dissociation on metal surfaces. Ideally, such calculations would treat all molecular degrees of freedom (DOFs) and the relevant surface DOFs without approximations. This is currently not possible, and the high-dimensional (i.e., modeling motion in many DOFs) QD calculations published so far rely on untested dynamical approximations [16, 22–24] and PESs based on untested density functionals [16, 22–24].

To help overcome these two shortcomings, we have performed *ab initio* molecular dynamics (AIMD) calculations and molecular beam experiments on the dissociation of CHD_3 on Pt(111) at normal incidence, comparing sticking (dissociation) probabilities of hyperthermal and CH-stretch excited CHD_3. The use of AIMD bypasses the need to fit a high-dimensional PES as forces are calculated on the fly with DFT, and allows motion to be described in all molecular DOFs as well as of the surface atoms, which should also be relevant: The minimum energy barrier to dissociative adsorption is considerably lowered if the surface atom below the dissociating molecule moves out of the surface plane [37], and the reaction shows a high surface temperature dependence [3, 38–41]. Our goal is to test the validity of the dynamical approximations and the density functionals used in earlier high-dimensional QD [16,22–24] and QCT [15,18,22] calculations on dissociation of methane on metal surfaces. Our calculations can help pave the way towards chemically accurate quantum dynamical calculations on reactions of methane on metal surfaces, as accomplished earlier for H_2 + Cu(111) [42].

5.2 Methods

AIMD calculations are performed with the VASP code [43–47]. The Pt surface is modeled with a 5 layer slab within a 3x3 supercell. A Γ-centered grid with 4x4x1 k-points samples the first Brillouin zone. Fermi smearing with a width of 0.1 eV has been used to facilitate convergence. The basis set includes plane waves up to a kinetic energy of 350 eV and core electrons have been represented with the projected augmented wave (PAW) method [47, 48] (see also Appendix 5.A.2). With the described computational setup, an equilibrium lattice constant of 3.975 Å has been obtained for bulk Pt, in reasonable agreement with the experimental value of 3.916 Å [49, 50].

In order to take the experimental surface temperature into account, a similar procedure as described in Ref. [51] and Chapter 3 has been followed: velocities and displacements from the equilibrium position have been assigned to surface atoms through an appropriate sampling and the optimized lattice constant has been expanded by 0.049% [49, 50] in order to simulate the platinum thermal expansion from 0 to 120 K, and by 0.386% for 0 to 500 K. These configurations are used in AIMD NVE simulations (constant number of atoms N, cell volume V and total energy E) to generate surface configurations for Monte-Carlo sampling, after which the molecule-surface collisions are simulated using NVE dynamics. Sticking probabilities are based on 1000 trajectories if the computed S_0 value is included in the range $1\% < S_0 < 10\%$, while 2000 and 500 trajectories have been computed for the $S_0 < 1\%$ and the $S_0 > 10\%$ cases, respectively. The dissociation probability values and their error bars (95% confidence interval unless otherwise stated) are evaluated using the Wilson (or score) method [52], which has been shown to provide a reasonable estimate of confidence intervals even for extremely low probabilities (close to 0%) [53], and which yields probabilities and standard deviations converging to the values obtained with the binomial distribution for large numbers of trajectories and probabilities.

The AIMD calculations we present use the QCT method. The usual QCT pitfalls (problems due to the absence of ZPE conservation and to neglect of tunneling effects) are avoided by performing the calculations for average total molecular energies $\langle E_{tot} \rangle$

E_b	E_b^c (CH_4)	E_b^c (CHD_2-D)	E_b^c (CD_3-H)
0.805	0.700	0.729	0.683

Table 5.1: Values of E_b and of E_b^c are given in eV for dissociation of CH_4 and CHD_3. The barrier geometry that we consider is computed from the minimum energy transition state configuration from Ref. [55].

well above E_b^c (the ZPE corrected value of E_b, see Table 5.1), and by avoiding reduced dimensionality calculations [22] (see also Appendix 5.A.3). The primary reason that we consider CHD_3 is that this allows us to also accurately study the effect of initial vibrational energy on the reactivity with the QCT method for the case that the ν_1 CH-stretch is pre-excited with one quantum. In CHD_3 the ν_1 CH-stretch is mostly localized on one bond and has a frequency that is off-resonance with other vibrations, so that artificial intra-molecular vibrational energy redistribution is minimized [54] (see Appendix 5.A.3). Compared to earlier QD and QCT calculations with a claim to high accuracy, advantages of the present AIMD calculations are that dynamical approximations [15, 16, 22–24], artificial energy flow between CH_4 vibrations of similar frequency [15, 18, 22], and errors in PES fitting [15, 16, 18, 22–24] are avoided, while the comparison of calculated laser-off reaction probabilities with experiment probes the quality of the density functional used more directly than other calculations [18].

Previously Sacchi et al. used AIMD to investigate the reaction of methane on Ni. However, they modeled the dynamics for the reverse associative desorption reaction, starting from the transition state towards the reactants (CH_4 + clean surface), invoking detailed balance in order to extract qualitative information regarding the relative efficacies of vibrational modes for promoting the forward dissociation reaction [19–21]. The present work is the first study using AIMD as a quantitative tool to compute probabilities for methane dissociation on a metal surface.

The GGA-level PBE density functional [56,57] has been used in the calculations. This makes our calculations relevant to earlier high-dimensional QD and QCT calculations on dissociation of methane on Ni and Pt surfaces: In these calculations, either the PW91 functional [58] was used [15, 16, 18] or the PBE functional, which was designed to reproduce PW91 energies [56], was used [18, 23, 24]. Boltzmann distributions of

vibrational states are used to describe the experimental gas temperature of the simulated laser-off beams. On the other hand, only molecules in the ($\nu_1 = 1$) initial state are considered when simulating laser-on beams, as appropriate. The initial conditions of each molecule are chosen such that normal vibrational coordinates and momenta sample classical microcanonical distributions. The initial molecular angular momentum is set to zero, and the initial E_i of the molecule samples velocity distributions as recorded experimentally using time-of-flight techniques. Details on the experimental techniques can be found in the Appendix 5.A.1. The experiments were done by the group of Rainer Beck at the EPFL (Lausanne, Switzerland)

5.3 Results and Discussion

We find semi-quantitative agreement between the theoretical and experimental dissociation probabilities (Figure 5.1). The calculations overestimate the experimental laser-off reactivity. The results therefore strongly suggest that the PBE functional used underestimates the E_b value (Table 5.1) for methane + Pt(111) by approximately 0.1 eV, this value being the energy with which the theoretical curve needs to be shifted in order to obtain agreement with experiment near the reaction threshold, while the E_b value obtained with the RPBE functional (1.06 eV [59]) is probably too high by 0.15 eV. These results are consistent with the finding that the PBE density functional typically overestimates and the RPBE functional usually underestimates the reactivity in activated dissociation of H_2 on metal surfaces [42, 60]. The value that our calculations suggest for E_b^c for CH_4 dissociating on Pt(111) (0.80 eV, i.e., our PBE value (Table 5.1) plus 0.1 eV), is consistent with an experimental estimate of this quantity (0.60 $\pm$ 0.20) eV. This estimate can be calculated [17] on the basis of calorimetry [28] and associative desorption experiments [29]. The agreement further improves if one considers that the barrier sampled in the desorption experiments (0.6 eV) is about 0.15 eV lower than the one sampled in adsorption (0.8 eV) due to lattice relaxation [55], i.e. the puckering of the Pt atom on which the methyl is adsorbed before desorption of methane.

Both experiment and theory show a large increase in the sticking probability when

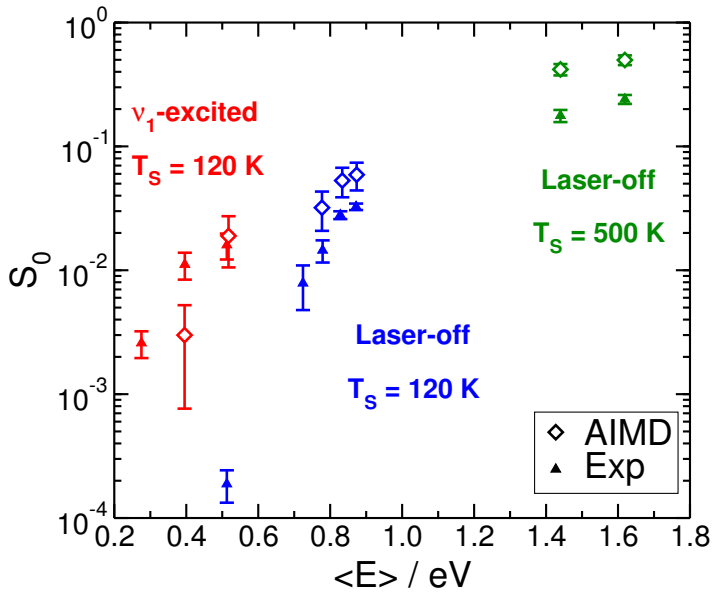

Figure 5.1: Sticking probability as a function of $\langle E_i \rangle$. Triangles are experimental and diamonds are AIMD results. Red symbols represent ν_1-excited beams, and blue symbols laser-off beams, both on a 120 K surface. Green symbols are for laser-off beams on a 500 K surface.

the CH-stretch mode is excited. Jiang et al. justified the observed enhancement in the CHD_3 + Ni(111) reactivity after pre-excitation of the ν_1 mode by considering the large projection that this mode has on the reaction coordinate at the transition state [15]. This argument, which is not specific to gas-surface reactions [61] and considered valid under the assumption that vibrational energy remains localized on the CH stretch, is expected to be valid for our system as well. Note that the theory underestimates the experimental vibrational efficacy, since the energy shift between the laser-off and the ν_1-excited reaction probability curves is lower for the AIMD results than for the experiments. One reason for this [62] could be that the barrier obtained with the PBE functional occurs at a too small value of the length of the breaking bond, as also found for H_2 + Cu(111) [42].

We analyzed the contribution of thermally excited vibrational states to the theoretical laser-off reactivity (Table 5.2). At the lowest E_i, the vibrationally excited molecules are 2.5 times more reactive than the ground state ones; this factor decreases with increasing

$\langle E_i \rangle$ (eV)	T_s (K)	T_n (K)	$P(v=0)$	$S_0^{v=0}$	$S_0^{v\neq 0}$	$S_0^{v\neq 0}/S_0^{v=0}$
0.78	120	836	42.4%	(1.8 ± 0.6) %	(4.4 ± 0.9) %	2.4
0.83	120	902	37.6%	(3.3 ± 0.9) %	(6.6 ± 1.0) %	2.0
0.87	120	971	29.4%	(3.9 ± 1.1) %	(6.9 ± 1.0) %	1.8
1.38	500	768	47.2 %	(34.3 ± 3.1) %	(48.5 ± 3.1) %	1.4
1.53	500	901	38.8 %	(49.5 ± 3.6) %	(50.0 ± 2.9) %	1

Table 5.2: Population and computed reactivity of ground state and vibrationally excited molecules in the laser-off simulations. $\langle E_i \rangle$ is the average translational energy, T_s is the surface temperature, T_n is the gas temperature in the expansion nozzle, $P(v=0)$ is the $v=0$ population and $S_0^{v=0}$ ($S_0^{v\neq 0}$) is the dissociation probability of the ground state (vibrationally excited) molecules in the thermally excited beams. Error bars represent 68.3 % confidence intervals.

	State	E_{tot}	%CD cleavage	% CH cleavage	% Error bars
AIMD	Laser-off	0.92	81.3	18.7	6.9
	Laser-off	1.00	77.4	22.6	5.7
	Laser-off	1.07	76.3	23.7	5.5
	$\nu_1 = 1$	0.77	0.0	100.0	24.9
	$\nu_1 = 1$	0.89	0.0	100.0	6.5
Experiment	Laser-off	0.55	71.4	28.6	-
	$\nu_1 = 1$	0.65	< 1	> 99	-

Table 5.3: Experimental and calculated branching ratios for different states and E_{tot} (eV). Error bars represent 68.3 % confidence intervals.

E_i. At the highest simulated E_i (1.53 eV), the reactivity of ground-state molecules is roughly equal to that of the vibrationally excited molecules. The larger effect of vibration at low E_i arises because at low E_i vibrational energy is needed to overcome the barrier for dissociation, whereas at higher E_i molecules already possess enough translational energy to dissociate.

The ratio between CH and CD bond cleavage is, within the error bars of the calculations, equal to the statistical value of 1:3 for laser-off beams, but only CH cleavage is observed when the CH-stretch is pre-excited (Table 5.3). This is in qualitative agreement with experiments, which were however done for lower E_{tot}, for which reaction probabilities could not be computed with AIMD. The reaction of vibrationally pre-excited CHD_3 is bond-selective because at the low E_i investigated vibrationless methane cannot react, so that the reaction should come from the vibrationally pre-excited normal mode, which in the present case is localized on the CH-stretch.

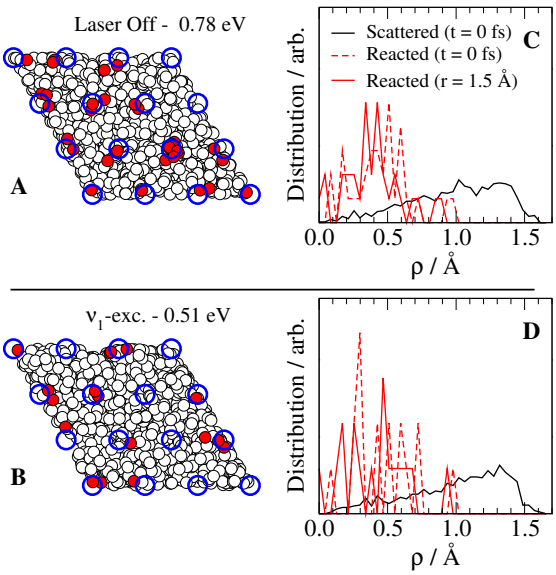

Figure 5.2: (A and B): Initial lateral displacement of the molecules in the supercell for two collision energies; red and white circles represent reacted and scattered molecules, respectively; blue open circles are the top sites in the supercell. (C and D): Impact parameter distributions for the collisions of the reacting molecules with the closest first layer atoms, evaluated at the beginning of the trajectories (dashed red line) and when the dissociating bond length reaches the lowest-energy transition-state value (solid red line). For comparison, the initial distributions of the scattered trajectories are plotted in black.

Insight into the microscopic details of the reaction and the validity of common dynamical approximations can be extracted from the collected dynamical data. For instance, we observe that dissociating molecules impact close to the top site (equilibrium position of a first layer atom, Figure 5.2), consistent with minimum energy paths for adsorption. The impact parameter distributions for collisions of normally incident CHD_3 with top layer surface atoms confirm this, and show that there is little steering towards reactive sites: the distributions do not shift much to lower impact parameters upon the approach of the reacting molecules to the transition state (Figure 5.2, panels C and D). This gives support to the use of sudden approximations [16, 23, 24], which assume that observables of interest can be computed by averaging results of calculations performed for fixed values of the coordinate(s) that remain almost unchanged, to describe the lateral motion of the molecule.

Angular distributions show that the initially non-rotating reacting molecules have their reactive bond initially pointing obliquely down to the surface, forming an angle with the surface normal in the range of $90° < \theta < 180°$ (Figure 5.3). During the subsequent approach to the barrier, there is little rotational steering (distributions only become a little bit narrower), and the distributions at the transition state are centered around values that are close to the orientation at the minimum energy barrier in the static calculations ($= 132.60°$) [37]. Molecules with small moments of inertia (high rotational constants) would be expected to easily reorient towards the minimum energy barrier orientation when approaching the transition state. Perhaps based on this argument, some of the earlier QD calculations [23, 24] employed the rotationally adiabatic approximation, which means that perfect steering of the reacting molecules was assumed along the reaction path. Our calculations show that this approximation is not valid for $CHD_3(\nu_1 = 1)$ because the initial distribution of the reacting molecules does not resemble a $\sin\theta$ distribution at all (the validity of this approximation for laser-off reaction has been discussed elsewhere [63]). In contrast, our result that the θ distributions at $t = 0$ and at the transition state are narrow and similar supports the use of the sudden approximation for the polar angle θ. In the light of the fairly large rotational constants of CHD_3 ($B = 3.3$ cm^{-1} and $C = 2.6$ cm^{-1} [64]) and our current findings, the sudden approximation is probably applicable to any direct gas-surface reaction of a polyatomic molecule under conditions similar as studied here. No correlation has been found between the reactivity and the azimuthal orientation of the dissociating bond (described by the ϕ angle), in agreement with observations of a flat PES with respect to ϕ in the static calculations [37].

In a similar analysis as used in earlier work that only allowed one-dimensional motion of a single surface atom [41], we looked at the time evolution of the vertical displacement of the surface atom closest to the incident molecule (Figure 5.4). Recoil is observed if the average is performed over scattered trajectories at all E_i, but for reactive trajectories recoil is only seen at high E_i. The profile for reactive trajectories at low E_i is different: reaction occurs only if the closest surface atom is above the surface plane and moves

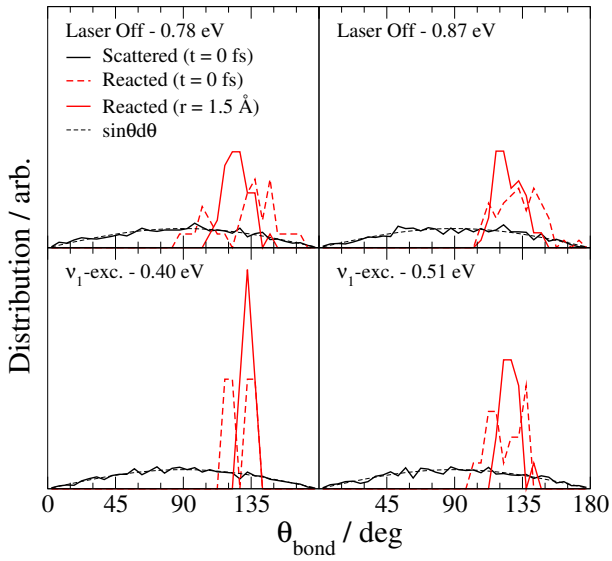

Figure 5.3: θ distributions evaluated at the beginning of the trajectories (dashed red line) and when the dissociating bond length reaches the lowest-energy transition-state value (solid red line) for reacting trajectories for four collision energies. For comparison, the distributions computed for the CH bonds of scattered trajectories are plotted in black. The dashed black lines correspond to $\sin\theta$, which is the distribution sampled when generating the initial orientations of the molecules.

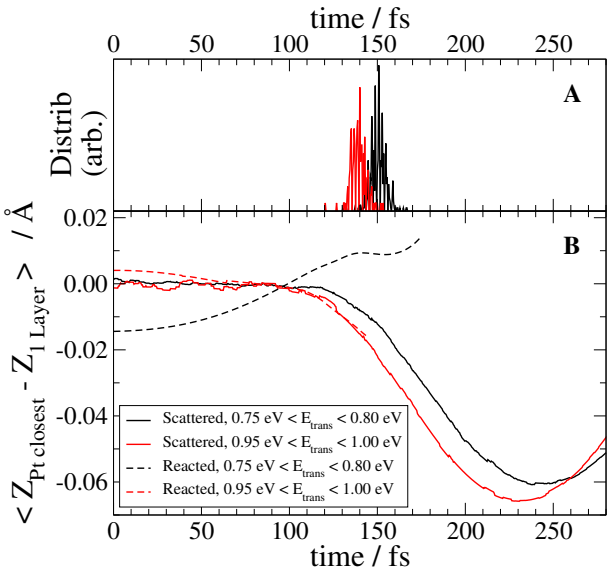

Figure 5.4: (A): Arrival distributions at the inner turning point in Z for scattered molecules for 0.75 eV $< E_i <$ 0.80 eV (black) and for 0.95 eV $< E_i <$ 1.00 eV (red). (B): Vertical displacement of the closest first layer atom as a function of time, averaged over scattered (solid lines) and reacted (dashed lines) laser-off trajectories in the two ranges of E_i (black and red, as in panel A).

towards the projectile, thereby lowering the barrier and increasing the relative velocity. At higher E_i reaction occurs regardless of the surface atom behaviour, and only recoil is seen [41]. Our AIMD results confirm the validity of the same result obtained earlier with models using a much more simplified treatment of surface motion [24, 38, 39, 41].

5.4 Summary and Conclusions

The AIMD method has been used for the first time to obtain quantitative results for the direct reaction of a polyatomic gas phase molecule colliding with a metal surface, in the form of statistically accurate reaction probabilities. The comparison of the AIMD results with new quantum-state resolved experiments on the reaction of CHD_3 with Pt(111), which is a prototypical example of such reactions, suggests that the AIMD method using the general purpose PBE functional is capable of a semi-quantitative description of this category of reactions. Somewhat surprisingly, even though methane has fairly large rota-

tional constants, our calculations suggest that a sudden approximation to the rotations should yield an accurate description of this reaction. This suggests a general applicability of the rotational sudden approximation to direct reactions of polyatomic molecules with surfaces for hyperthermal energies. The suitability of the sudden approximation for describing the lateral motion of the methane molecule, and the active role played by the surface atom motion in the dissociation dynamics at low collision energies, which have been previously put forward for similar systems (Refs. [16,23,24] and Refs. [24,38,39,41], respectively), have been confirmed by the current study. The AIMD calculations also reproduce the observed bond-selectivity in the dissociation of CH-stretch pre-excited CHD_3, and they suggest that the PBE functional underestimates the reaction barrier height by ≈ 0.1 eV for CH_4 + Pt(111). The latter finding, and similar observations for H_2 + Cu(111) and Ru(0001), suggest that the PBE and PW91 functionals, which were used in earlier high-dimensional QD and QCT calculations on methane dissociation on Ni and Pt surfaces, underestimate the barriers for these systems by a similar amount.

5.A Appendix

5.A.1 Experimental Methods

Quantum state resolved dissociation probabilities of CHD_3 on Pt(111) were measured in a molecular beam/surface science apparatus described previously [27, 65]. Reflection absorption infrared spectroscopy (RAIRS) was used to detect the nascent dissociation products CD_3(ads) and CHD_2(ads) of CHD_3 on the cold Pt(111) surface ($T_s = 120$ K) in order to measure both the absolute dissociation probability (S_0) and the branching ratio of the C-H and C-D cleavage channels with and without state specific laser preparation of the incident CHD_3. For the laser-off measurements above 0.7 eV incident energy, where the dissociation coefficient exceeds 1%, the King&Wells beam reflectivity technique [66] was used to measure absolute sticking coefficients of CHD_3 on Pt(111). With this method, the branching ratio could not be measured.

Molecular beam parameters are supplied in Table 5.A.1. The stream velocity (v_s) and the width parameter (α) of the beams have been obtained by fitting a flux-weighted velocity distribution (Equation 4 of Ref. [67]) to recorded TOF spectra.

5.A.2 Convergence Tests

Table 5.A.2 shows the convergence of our computational setup in the evaluation of the energy barrier (E_b) for CH_4 + Pt(111). E_b is calculated as $E_{b,abs} - E_\infty$, where E_∞ is the energy of the system with the CH_4 molecule in its equilibrium geometry at large distance from the ideal metal slab and $E_{b,abs}$ is the absolute barrier energy, computed for the minimum energy transition state configuration (the D1 configuration in figure 3 of Ref. [55]). The calculations with a 2x2 surface unit cell show that converged results may be obtained with 5 layers. The calculations with 5 layers show that converged results may be obtained with a 3x3 surface unit cell. We estimate that, with our computational setup, the PBE value of E_b is converged to within 1 kcal/mol (43 meV).

Translational Energy (eV)	Total Energy (eV)	State	Set Nozzle Temperature (K)	Gas Temperature (K)	v_s (m/s)	α (m/s)
0.514	0.552	Laser-off	500	534	2263	156
0.727	0.837	Laser-off	700	764	2679	227
0.781	**0.919**	**Laser-off**	**750**	**836**	**2774**	**248**
0.830	**0.997**	**Laser-off**	**800**	**902**	**2857**	**265**
0.875	**1.074**	**Laser-off**	**850**	**971**	**2926**	**291**
1.376	**1.487**	**Laser-off**	**700**	**768**	**3739**	**417**
1.535	**1.7016**	**Laser-off**	**800**	**901**	**3948**	**482**
0.276	0.648	$\nu_1 = 1$	-	300	1662	98
0.397	**0.769**	$\nu_1 = 1$	**400**	**412**	**1992**	**122**
0.514	**0.886**	$\nu_1 = 1$	**500**	**534**	**2263**	**156**

Table 5.A.1: Molecular beam parameters. v_s and α represent the stream velocity and the width parameter of the beams, respectively. The beams which have been simulated using AIMD have been highlighted.

Surface Unit Cell Size	Number of Atomic Layers	k-point grid	Cut-off energy (eV)	E_b (eV)
2x2	4	8x8x1	350	0.926
2x2	4	8x8x1	400	0.931
2x2	4	8x8x1	600	0.933
2x2	4	16x16x1	350	0.928
2x2	5	8x8x1	350	0.872
2x2	10	8x8x1	350	0.885
3x3	4	6x6x1	350	0.887
3x3	**5**	**4x4x1**	**350**	**0.805**
3x3	5	4x4x1	500	0.811
3x3	5	8x8x1	350	0.813
4x4	4	4x4x1	350	0.861
4x4	5	4x4x1	500	0.801

Table 5.A.2: Convergence tests of the electronic structure calculations for CH_4 + Pt(111). The barrier energy E_b has been computed varying the surface unit cell size, the number of atomic layers in the slab, the k-point grid size (Γ-point is always included) and the cut-off energy for the plane waves expansion. The energy barrier of our computational setup has been highlighted.

5.A.3 Avoiding the Pitfalls of the Quasi-Classical Trajectory (QCT) Method

5.A.3.1 Zero Point Energy (ZPE) Conservation Problems

Calculations for D_2 + Cu(111) show that, if motion in all molecular DOFs is modeled for average total energies of the molecule $\langle E_{tot} \rangle$ above the ZPE-corrected minimum barrier height (E_b^c), QCT calculations essentially reproduce the quantum dynamics (QD) results [68]. We therefore expect that ZPE conservation problems, which may hamper the accurate calculation of reaction probabilities near the reaction threshold if some of the coordinates are kept frozen or treated with other dynamical approximations [22, 69], will not much affect the accuracy of our calculations, which are all done for $\langle E_{tot} \rangle$ well above E_b^c (Table 5.1).

To make sure that ZPE conservation problems have no significant effect on our calculations, we looked at whether evidence of ZPE violation could be found in our actual AIMD calculations. No strong proof of ZPE violation has been found in the dynamics as a possible reason of the too high reaction probability even at low average incidence energy $\langle E_i \rangle$: the available energy to the reaction (the sampled E_{tot}) is larger than the ZPE-corrected minimum energy barrier from static calculations, in almost all (i.e., 143) of the 144 reacted trajectories computed in total for the three lowest $\langle E_i \rangle$ laser-off simulations, and in all of the laser-on reacted trajectories. Furthermore, the reaction probability is overestimated even at the highest $\langle E_i \rangle$, where the experimental reaction probabilities are larger than 15% and ZPE violation is not expected to play a role.

5.A.3.2 Artificial Intramolecular Vibrational Energy Redistribution (IVR)

In order to avoid the potential problem of artificial energy flow among vibrations alluded to above, we focus on two types of experiment. The first ('laser-off') experiment addresses the reactivity of CHD_3 in a hyperthermal supersonic beam, in which the vibrational ground state has the highest population. In the second type of experiment the ν_1 (CH-stretch) mode is pre-excited with one quantum but due to the localization of the

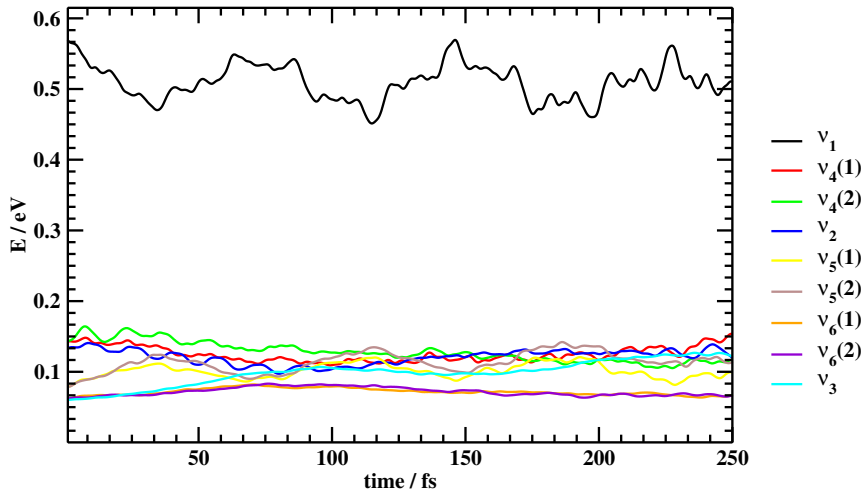

Figure 5.A.1: The normal mode energies are plotted as a function of time for freely vibrating CH-stretch (ν_1, in black) excited CHD_3. The energies plotted here are the result of an average over 100 trajectories.

vibrational mode on the CH bond, this mode is off-resonance with other vibrations, so that artificial intra-molecular vibrational energy redistribution (IVR) is minimized [54]. We carefully verified that AIMD is able to simulate freely vibrating CH-stretch (ν_1) excited CHD_3 without significant energy 'leakage' from the ν_1 mode to others. Figure 5.A.1 shows the normal mode energies as a function of time, averaged over 100 trajectories for which the initial conditions (normal mode vibrational coordinates and velocities) sample classical microcanonical distributions. The normal mode energies have been evaluated by projecting the vibrational coordinates of CHD_3 onto its equilibrium normal mode coordinates. As evident from Figure 5.A.1, the vibrational energy imparted to the ν_1 mode remains localized in this vibrational mode on the time-scale of the collisions in our simulations (100-200 fs).

5.A.3.3 Role of Tunneling

Early on, it was argued that an exponential dependence of the dissociation probability on E_i observed in supersonic molecular beam experiments between $E_i = 0.70$ to 0.98 eV should be due to tunneling, on the basis of a one-dimensional model [25]. However, this model implied a very high ZPE-corrected barrier height of 1.25 eV, whereas experiments

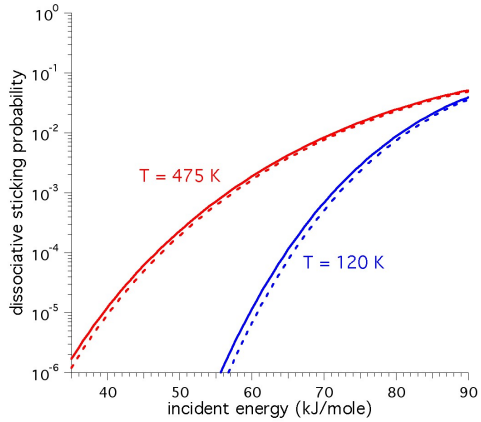

Figure 5.A.2: Dissociative sticking probability as a function of incident energy for vibrationally ground state CH_4 incident on Ni(100) at the temperatures indicated. The curves are from the reaction path model described in Ref. [23], for the case where the vibrationally non-adiabatic couplings are set equal to zero. The dashed lines exclude contributions to the sticking from tunneling. The results reported for $T_s = 475$ K are from Ref. [23].

suggest a value of only 0.6 ± 0.2 eV [17].

Even though we use it here for a different surface (Ni(100)), the reaction path Hamiltonian model described in Ref. [23] allows an estimate to be made of the tunneling contribution for the lowest surface temperature (T_s) considered in our calculations on CHD_3+Pt(111). The reaction probability has been computed by averaging the results of one-dimensional (1D) quantum dynamics calculations over surface sites and a surface atom coordinate, after setting all the vibrationally non-adiabatic couplings to zero (see figure 9 of Ref. [23] and the corresponding more detailed discussion in Ref. [23]). The tunneling contribution can be excluded by setting all the 1D reaction probabilities ≤ 0.5 equal to zero. The reaction probability curves including and excluding tunneling contributions are plotted in Figure 5.A.2. The two curves are displaced from one another along the energy axis by less than 1 kJ/mol (0.01 eV) when $S_0 = 10^{-3}$ for $T_s = 120$ K.

Since we only simulate conditions for which the experimental reaction probabilities are > 0.01, we do not expect that the neglect of tunneling effects in our calculations has a large effect on our most important conclusions. In particular, the neglect of tunneling should hardly affect our conclusion regarding the barrier height for CHD_3 + Pt(111),

the conclusion being that the PBE functional underestimates this quantity by 0.1 eV. This does not mean that tunneling does not influence the reaction: at the incidence energy where the quantum mechanical reaction probability is 0.01 (80.5 kJ/mol $\approx$ 0.83 eV), the tunneling contribution to the reaction is approximately 10% (i.e., the tunneling contribution to the reaction probability is approximately 0.001). The reason that the tunneling contribution is so low for this low incidence energy (for Ni(100) the zero-point energy corrected barrier height for the static surface is 0.78 eV [55]) is that even at T_s = 120 K excited surface vibrational states are populated, and this allows reaction through a classical over the barrier mechanism because the outward motion of the surface atom above which methane reacts lowers the reaction barrier [55].

The comparison of calculations on reaction of a supersonic beam of CH_4 with Pt(111) at $E_i = 0.62$ eV and $T_s = 200$ K [70], which used a statistical model and either included [17] or excluded [30] the effect of tunneling, likewise suggests only a minor role for tunneling under the conditions addressed by us.

Finally, we also expect no problems due to neglect of tunneling with computing branching ratios for CHD_3 dissociation into CD_3 + H and CHD_2 + D, as a recent QCT study was able to show that the strong kinetic isotope effect observed previously when comparing CH_4 to CD_4 dissociation on Pt(111) [3] could be explained on the basis of the molecules' different ZPEs [18].

Bibliography

[1] G. Jones, J. G. Jakobsen, S. S. Shim, J. Kleis, M. P. Andersson, J. Rossmeisl, F. Abild-Pedersen, T. Bligaard, S. Helveg, B. Hinnemann, J. R. Rostrup-Nielsen, I. Chorkendorff, J. Sehested, and J. K. Nørskov, J. Catal. **259**, 147 (2008).

[2] L. B. F. Juurlink, D. R. Killelea, and A. L. Utz, Prog. Surf. Sci. **84**, 69 (2009).

[3] A. C. Luntz and D. S. Bethune, J. Chem. Phys. **90**, 1274 (1989).

[4] C. T. Rettner, H. E. Pfnür, and D. J. Auerbach, J. Chem. Phys. **84**, 4163 (1986).

[5] R. D. Beck, P. Maroni, D. C. Papageorgopoulos, T. T. Dang, M. P. Schmid, and T. R. Rizzo, Science **302**, 98 (2003).

[6] L. B. F. Juurlink, P. R. McCabe, R. R. Smith, C. L. DiCologero, and A. L. Utz, Phys. Rev. Lett. **83**, 868 (1999).

[7] P. Maroni, D. C. Papageorgopoulos, M. Sacchi, T. T. Dang, R. D. Beck, and T. R. Rizzo, Phys. Rev. Lett. **94**, 246104 (2005).

[8] J. Higgins, A. Conjusteau, G. Scoles, and S. L. Bernasek, J. Chem. Phys. **114**, 5277 (2001).

[9] L. Halonen, S. L. Bernasek, and D. J. Nesbitt, J. Chem. Phys. **115**, 5611 (2001).

[10] R. R. Smith, D. R. Killelea, D. F. DelSesto, and A. L. Utz, Science **304**, 992 (2004).

[11] D. R. Killelea, V. L. Campbell, N. S. Shuman, and A. L. Utz, Science **319**, 790 (2008).

[12] L. Chen, H. Ueta, R. Bisson, and R. D. Beck, Faraday Discuss. **157**, 285 (2012).

[13] B. L. Yoder, R. Bisson, and R. D. Beck, Science **329**, 553 (2010).

[14] M. B. Lee, Q. Y. Yang, and S. T. Ceyer, J. Chem. Phys. **87**, 2724 (1987).

[15] B. Jiang and H. Guo, J. Phys. Chem. C **117**, 16127 (2013).

[16] B. Jiang, R. Liu, J. Li, D. Xie, M. Yang, and H. Guo, Chem. Sci. **4**, 3249 (2013).

[17] S. B. Donald, J. K. Navin, and I. Harrison, J. Chem. Phys. **139**, 214707 (2013).

[18] X. J. Shen, A. Lozano, W. Dong, H. F. Busnengo, and X. H. Yan, Phys. Rev. Lett. **112**, 046101 (2014).

[19] M. Sacchi, D. J. Wales, and S. J. Jenkins, J. Phys. Chem. C **115**, 21832 (2011).

[20] M. Sacchi, D. J. Wales, and S. J. Jenkins, Phys. Chem. Chem. Phys. **14**, 15879 (2012).

[21] M. Sacchi, D. J. Wales, and S. J. Jenkins, Comput. Theor. Chem. **990**, 144 (2012).

[22] M. Mastromatteo and B. Jackson, J. Chem. Phys. **139**, 194701 (2013).

[23] B. Jackson and S. Nave, J. Chem. Phys. **135**, 114701 (2011).

[24] B. Jackson and S. Nave, J. Chem. Phys. **138**, 174705 (2013).

[25] G. Schoofs, C. Arumainayagam, M. Master, and R. Madix, Surf. Sci. **215**, 1 (1989).

[26] R. Bisson, M. Sacchi, T. Dang, B. Yoder, P. Maroni, and R. Beck, J. Phys. Chem. A **111**, 12679 (2007).

[27] L. Chen, H. Ueta, R. Bisson, and R. D. Beck, Rev. Sci. Instrum. **84**, 053902 (2013).

[28] E. M. Karp, T. L. Silbaugh, and C. T. Campbell, J. Am. Chem. Soc. **135**, 5208 (2013).

[29] F. Zaera, Surf. Sci. **262**, 335 (1992).

[30] S. B. Donald and I. Harrison, Phys. Chem. Chem. Phys. **14**, 1784 (2012).

[31] B. Ølgaard Nielsen, A. C. Luntz, P. M. Holmblad, and I. Chorkendorff, Catal. Lett. **32**, 15 (1995).

[32] G. J. Kroes, Phys. Chem. Chem. Phys. **14**, 14966 (2012).

[33] J. Zheng, Y. Zhao, and D. G. Truhlar, J. Chem. Theory Comput. **5**, 808 (2009).

[34] R. Peverati and D. G. Truhlar, Phil. Trans. R. Soc. A **372**, 20120476 (2014).

[35] M. Wijzenbroek and G. J. Kroes, J. Chem. Phys. **140**, 084702 (2014).

[36] J. Greeley, J. Nørskov, and M. Mavrikakis, Annu. Rev. Phys. Chem. **53**, 319 (2002).

[37] S. Nave and B. Jackson, J. Chem. Phys. **130**, 054701 (2009).

[38] S. Nave and B. Jackson, J. Chem. Phys. **127**, 224702 (2007).

[39] S. Nave and B. Jackson, Phys. Rev. Lett. **98**, 173003 (2007).

[40] A. K. Tiwari, S. Nave, and B. Jackson, Phys. Rev. Lett. **103**, 253201 (2009).

[41] A. K. Tiwari, S. Nave, and B. Jackson, J. Chem. Phys. **132**, 134702 (2010).

[42] C. Díaz, E. Pijper, R. A. Olsen, H. F. Busnengo, D. J. Auerbach, and G. J. Kroes, Science **326**, 832 (2009).

[43] G. Kresse and J. Hafner, Phys. Rev. B **47**, 558 (1993).

[44] G. Kresse and J. Hafner, Phys. Rev. B **49**, 14251 (1994).

[45] G. Kresse and J. Furthmüller, Comput. Mat. Sci. **6**, 15 (1996).

[46] G. Kresse and J. Furthmüller, Phys. Rev. B **54**, 11169 (1996).

[47] G. Kresse and D. Joubert, Phys. Rev. B **59**, 1758 (1999).

[48] P. E. Blöchl, Phys. Rev. B **50**, 17953 (1994).

[49] J. W. Arblaster, Platinum Met. Rev. **41**, 12 (1997).

[50] J. W. Arblaster, Platinum Met. Rev. **50**, 118 (2006).

[51] F. Nattino, C. Díaz, B. Jackson, and G. J. Kroes, Phys. Rev. Lett. **108**, 236104 (2012).

[52] E. B. Wilson, J. Am. Statist. Assoc. **22**, 209 (1927).

[53] A. Agresti and B. A. Coull, Am. Stat. **52**, 119 (1998).

[54] Z. Xie, J. M. Bowman, and X. Zhang, J. Chem. Phys. **125**, 133120 (2006).

[55] S. Nave, A. K. Tiwari, and B. Jackson, J. Chem. Phys. **132**, 054705 (2010).

[56] J. P. Perdew, K. Burke, and M. Ernzerhof, Phys. Rev. Lett. **77**, 3865 (1996).

[57] J. P. Perdew, K. Burke, and M. Ernzerhof, Phys. Rev. Lett. **78**, 1396 (1997).

[58] J. P. Perdew, J. A. Chevary, S. H. Vosko, K. A. Jackson, M. R. Pederson, D. J. Singh, and C. Fiolhais, Phys. Rev. B **46**, 6671 (1992).

[59] F. Viñes, Y. Lykhach, T. Staudt, M. P. A. Lorenz, C. Papp, H. P. Steinrück, J. Libuda, K. M. Neyman, and A. Görling, Chem. - Eur. J. **16**, 6530 (2010).

[60] P. Nieto, D. Farías, R. Miranda, M. Luppi, E. J. Baerends, M. F. Somers, M. J. T. C. van der Niet, R. A. Olsen, and G. J. Kroes, Phys. Chem. Chem. Phys. **13**, 8583 (2011).

[61] F. F. Crim, Proc. Natl. Acad. Sci. U. S. A. **105**, 12654 (2008).

[62] D. Halstead and S. Holloway, J. Chem. Phys. **93**, 2859 (1990).

[63] B. Jackson, F. Nattino, and G. J. Kroes, J. Chem. Phys. **141**, 054102 (2014).

[64] C. Roche, J. P. Champion, and A. Valentin, J. Mol. Spectrosc. **160**, 517 (1993).

[65] H. Ueta, L. Chen, R. D. Beck, I. Colon-Diaz, and B. Jackson, Phys. Chem. Chem. Phys. **15**, 20526 (2013).

[66] D. A. King and M. G. Wells, Proc. R. Soc. Lond. A-Math. Phys. Sci. **339**, 245 (1974).

[67] H. A. Michelsen and D. J. Auerbach, J. Chem. Phys. **94**, 7502 (1991).

[68] C. Díaz, R. A. Olsen, D. J. Auerbach, and G. J. Kroes, Phys. Chem. Chem. Phys. **12**, 6499 (2010).

[69] G. R. Darling, Z. S. Wang, and S. Holloway, Phys. Chem. Chem. Phys. **2**, 911 (2000).

[70] J. Harris, J. Simon, A. C. Luntz, C. B. Mullins, and C. T. Rettner, Phys. Rev. Lett. **67**, 652 (1991).